ORIGINAL RESEARCH ARTICLE

Autophagy inhibition via *Becn1* downregulation improves the mesenchymal stem cells antifibrotic potential in experimental liver fibrosis

Hang Yu Wang[1] | Can Li[2,3] | Wei Hua Liu[3] | Feng Mei Deng[2,3] | Yan Ma[4] |
Li Na Guo[2] | De Hua Kong[3] | Kang An Hu[3] | Qin Liu[3] | Jiang Wu[5] | Jing Sun[2,3] |
Yi Lun Liu[3,4]

[1]Key Laboratory of Xingjiang Phytomedicine Resources and Utilization, Ministry of Education, School of Pharmacy, Shihezi University, Shihezi, China

[2]Department of Pathology and Pathophysiology, Chengdu Medical College, Chengdu, China

[3]Sichuan Clinical Research Center for Geriatrics, The First Affiliated Hospital of Chengdu Medical College, Chengdu, China

[4]Department of Surgery, The First Affiliated Hospital of Chengdu Medical College, Chengdu, China

[5]Deep-Underground Medicine Laboratory, West China Hospital of Sichuan University, Chengdu, China

Correspondence
Jing Sun, Department of Pathology and Pathophysiology, Chengdu Medical College, 783 Xindu Avenue, Chengdu 610500, China.
Email: jingsunn@126.com

Yi L. Liu, Sichuan Clinical Research Center for Geriatrics, The First Affiliated Hospital of Chengdu Medical College, 278 Bao Guang Avenue, Chengdu 610500, China.
Email: yilunliu@foxmail.com

Abstract

Liver fibrosis (LF) is the result of a vicious cycle between inflammation-induced chronic hepatocyte injury and persistent activation of hepatic stellate cells (HSCs). Mesenchymal stem cell (MSC)-based therapy may represent a potential remedy for treatment of LF. However, the fate of transplanted MSCs in LF remains largely unknown. In the present study, the fate and antifibrotic effect of MSCs were explored in a LF model induced by CCl_4 in mouse. Additionally, MSCs were stimulated in vitro with LF-associated factors, tumor necrosis factor-α (TNF-α), interferon-γ (IFN-γ), and transforming growth factor-β1 (TGF-β1), to mimic the LF microenvironment. We unveiled that MSCs exhibited autophagy in response to the LF microenvironment through *Becn1* upregulation both in vivo and in vitro. However, autophagy suppression induced by *Becn1* knockdown in MSCs resulted in enhanced antifibrotic effects on LF. The improved antifibrotic potential of MSCs may be attributable to their inhibitory effects on T lymphocyte infiltration, HSCs proliferation, as well as production of TNF-α, IFN-γ, and TGF-β1, which may be partially mediated by elevated paracrine secretion of PTGS2/PGE$_2$. Thus, autophagy manipulation in MSCs may be a novel strategy to promote their antifibrotic efficacy.

KEYWORDS
autophagy, hepatic stellate cells, immunosuppression, liver fibrosis, mesenchymal stem cells

----

1 | INTRODUCTION

Liver fibrosis (LF), characterized by extracellular matrix (ECM) protein production and accumulation, is a vicious cycle between chronic inflammation-induced persistent parenchymal cell injury and activation of consequent wound-healing responses executed mainly by activated myofibroblasts, which define the LF microenvironment (Tsuchida & Friedman, 2017). Genetic techniques have provided strong evidence that primed hepatic stellate cells (HSCs) are the prominent cellular origin of matrix protein-secreting myofibroblasts (Lee, Wallace, & Friedman, 2015; Trautwein, Friedman, Schuppan, & Pinzani, 2015). Genetic lineage-tracing analysis performed by Kramann et al. (2015) strongly suggested that glioma-associated oncogene homolog 1 (*Gli1*) is an in vivo marker of myofibroblast progenitors; thus, HSCs can be traced in vivo using a *Gli1* genetic lineage-tracing technique. In addition, both the occurrence and progression of LF are closely related to T-cell-mediated immune responses (Pesce et al., 2006; Wynn, 2004).

Multiple researches have consolidated the beneficial efficacy of mesenchymal stem cells (MSCs) on treatment of varied inflammatory disease (L. Bai et al., 2012; Rocheteau et al., 2015; Swart et al., 2015), and the therapeutic effects of MSCs are largely attributable to their profound immunoinhibitive capacity (Horton et al., 2013; Wang, Chen, Cao, & Shi, 2014). Nevertheless, the uncertainty of the transplanted MSCs poses critical challenge for obtaining predictable therapeutic effects in vivo. The in vivo inflammatory microenvironment is a pivotal necessity for MSCs to execute their immunomodulatory functions (Ren et al., 2008). The interactions between MSCs and inflammatory microenvironment regulate the immunomodulatory properties of MSCs (Y. Liu et al., 2011). However, few studies have evaluated the mechanisms through which the inflammatory microenvironment of LF controls the immunoregulatory capability of MSCs.

Autophagy is a highly conservative eukaryotic degradative process, which is a requisite for replying and adapting to environmental alterations (Cadwell, 2016). Autophagy-related genes (*Atgs*), including *Atg7*, *Atg12*, *Atg5* as well as *Becn1*, regulate autophagosome maturation (Antonioli, Di Rienzo, Piacentini, & Fimia, 2017). Emerging evidence has confirmed a close link between autophagy and immunomodulation has been confirmed by emerging evidence (Shibutani, Saitoh, Nowag, Münz, & Yoshimori, 2015). Some studies unveiled that inflammatory microenvironment hindered the immunosuppressive properties of MSCs by priming autophagy (Dang et al., 2014). Therefore, we hypothesized that the LF microenvironment could also interact with the autophagic and immunoregulatory potential of MSCs and that modulation of autophagy may in turn influence the therapeutic effect of MSCs in LF.

In the current study, we assessed the autophagy activity in transplanted MSCs triggered by hepatic microenvironment in vivo. We also examined the effect of stimulating MSCs by LF-related cytokines, including tumor necrosis factor (TNF)-α, interferon-γ (IFN-γ), and transforming growth factor-β1 (TGF-β1) on autophagy-related gene expression. Furthermore, we evaluated the effect of autophagy

inhibition on the antifibrotic activity of MSCs. The findings of this study are expected to provide novel insights into the relationship between autophagy and the immunomodulatory effects of MSCs, and indicate whether autophagy could be considered as a promising therapeutic target for MSCs for treating LF.

2 | MATERIALS AND METHODS

2.1 | Isolation and culture of MSCs

MSCs were enriched from the bone marrow of male C57BL/6 mice and cultured in DMEM-low glucose (cat. no. 01-051-1AC5; BI, Kibbutz Beit Haemek, Israel) containing 10% fetal bovine serum (FBS, cat. no. 10099-141; Gibco, Grand Island, NY). MSCs were seeded at 2×10^6 cells/100-mm culture dish (cat. no. 07-3100; Biologix Group, Jiangsu, China) and cultured for 72 hr in an incubator containing 5% CO_2 at 37°C. To remove floating cells, on the second day, the cultures were rinsed twice with phosphate-buffered saline (PBS). The methods for MSC characterization are described in the Supporting Information Materials. Phenotypic characterization of MSCs is presented in Supporting Information Data.

2.2 | Short hairpin RNA (shRNA)-mediated *Becn1* stable knockdown

The specific *Becn1* shRNA was purchased from Geneplay Biomedical Technology (Suzhou, China). The nucleotide sequences were as follows: Plko.1-EGFP-*Becn1*-shRNA, 5′-GGAGAAAGGCAAGATTGAA GA-3′; scrambled control (shNC), 5′-CCTAAGGTTAAGTCGCCCT CG-3′. A multiplicity of infection of 200 of lentiviruses was utilized for MSC infection.

2.3 | In vitro MSC treatment

MSCs were starved or treated with TNF-α (20 ng/ml, cat. no. 50349-MNAE; SB, Beijing, China), IFN-γ (50 ng/ml, cat. no. 50709-MNAH; SB), or TGF-β1 (10 ng/ml, cat. no. 7666-MB-005; R&D Systems, Minneapolis, MN) for 0–24 hr and then subjected to western blot analysis of microtubule-associated protein 1A/1B light chain 3 (MAP1LC3). Cells incubated under starvation served as a positive control. MSCs were stimulated with TNF-α (20 ng/ml), IFN-γ (50 ng/ml), and TGF-β1 (10 ng/ml) alone or in different combinations for 6 hr. Subsequently, MAP1LC3-I, MAP1LC3-II, and p62 expression levels were measured using western blot analysis. Autophagosome formation was detected by transmission electron microscopy, and MAP1LC3 dot formation in MSCs was visualized by immunofluorescence staining. Additionally, shNC-MSCs and sh*Becn1*-MSCs were incubated in absence or presence of TNF-α (20 ng/ml), IFN-γ (50 ng/ml), or TGF-β1 (10 ng/ml) for 6 hr. Subsequently, *Becn1* messenger RNA (mRNA) levels were measured by quantitative reverse transcription polymerase chain reaction (qRT-PCR). In addition, protein expression levels of MAP1LC3-I, MAP1LC3-II, p62, and BECN1 were detected using immunoblotting. To further evaluate the

effects of *Becn1* knockdown on expression of prostaglandin-endoperoxide synthase 2 (PTGS2) in MSCs, shNC-MSCs were treated with or without 3-methyladenine (3-MA, cat. no. M9281; Sigma, St. Louis, MO), and sh*Becn1*-MSCs were incubated for indicated time with or without rapamycin (cat. no. 553210; Sigma) under stimulation with TNF-α (20 ng/ml), IFN-γ (50 ng/ml), and TGF-β1 (10 ng/ml) for 12 hr.

2.4 | Transmission electron microscopy

After starvation or combined treatment of TNF-α, IFN-γ, and TGF-β1, MSCs were rinsed with PBS and fixed with 2% glutaraldehyde (cat. no. G5882; Sigma) in 0.1 M phosphate buffer (pH 7.2) for 2 hr at 4°C. The cells were postfixed with 1% osmic acid for another 2 hr at 4°C, followed by dehydration using ethanol in graded concentrations. Subsequently, the sections were incubated with uranylacetate and lead citrate (cat. no. 15326; Sigma), and images were acquired using an Olympus EM208S transmission electron microscope (Olympus, Tokyo, Japan).

2.5 | LF model induction and MSC transplantation

Male SPF C57BL/6 mice (2 months of age, average body weight: 25 g) were obtained from Chengdu Dossy Experimental Animals Co. Ltd. (Chengdu, China). *Gli1*CreER^{t2} (cat. no. 007913) and Rosa26*tdTomato* (cat. no. 007909) mice were obtained from Jackson Laboratories (Bar Harbor, ME). For lineage-tracing studies, 6–7-week-old male mice underwent three intraperitoneal injections of tamoxifen (cat. no. 06734; Sigma) at a dose of 0.1 mg/kg body weight in corn oil/3% ethanol 10 days before LF induction. Detailed information on identification of *Gli1* genetic lineage-tracing mice is given in the Supporting Information Materials. LF mice were induced by CCl_4 olive oil solution (CCl_4:olive oil = 1:3) via intraperitoneal injection at a concentration of 4 ml/kg twice per week for 5 consecutive weeks (CCl_4 mice). Accordingly, the control group mice were then subjected to the same concentration of olive oil by intraperitoneal injection (oil mice).

    MSCs of passage 5 (P5) infected with lentivirus-control shRNA were transplanted into oil mice and CCl_4 mice at a density of 1×10^6 cells in 100 μl normal saline per mouse via the tail vein (on Week 5, $n = 8$). Mice were euthanized at 0 and 72 hr after cell administration. In subsequent in vivo experiments, 32 mice were randomly designated into four groups with comparable mean body weights; the groups were as follows: oil + PBS, CCl_4 + PBS, CCl_4 + shNC, and CCl_4 + sh*Becn1* groups ($n = 8$ each). In the CCl_4 + PBS, CCl_4 + shNC, and CCl_4 + sh*Becn1* groups, CCl_4-induced LF model mice were subjected to weekly administration of PBS, shNC-MSCs (1×10^7/ml, P5), or sh*Becn1*-MSCs (1×10^7/ml, P5) from Weeks 3 to 5 via the tail vein. The oil + PBS group underwent PBS administration with the same volume and sequence as the treatment group after oil treatment. The mice were killed 3 days after cell transplantation. In some in vivo experiments, 32 mice were randomly allocated to four groups, that is, oil + shNC, oil + sh*Becn1*, CCl_4 + shNC, and CCl_4 +

sh*Becn1* groups ($n = 8$ each). shNC-MSCs or sh*Becn1*-MSCs were administered to oil mice or CCl_4 mice (on Week 5) via tail vein. The mice were euthanized 3 days after cell transplantation for subsequent evaluation of the localization of exogenous MSCs in the liver.

    All animal operations were conducted in line with the Chinese Guidelines for Use of Experimental Animals, which was also approved by the Animal Experimentation Ethics Committee, the First Affiliated Hospital of Chengdu Medical College, China.

2.6 | Sirius red, Masson, and hematoxylin and eosin (HE) staining

After being injected with PBS, shNC-MSCs, or sh*Becn1*-MSCs, mice were euthanized and liver tissues were obtained. The liver tissues were embedded in paraffin following alcohol dehydration. Sections of liver were then subjected to HE staining (cat. no. KGA224; KeyGEN BioTECH, Nanjing, China), Masson staining (cat. no. HT15-1KT; Sigma), or Sirius red staining (cat. no. G1471; Solarbio).

2.7 | Immunofluorescence staining

Mice were euthanized, and livers were resected, embedded into OCT (cat. no. 4583; Sakura), and stored at −80°C. Following cutting, frozen sections were permeabilized using 0.5% Triton X-100 (cat. no. ST795; Beyotime, Shanghai, China) and blocked with 5% bovine serum albumin (BSA, cat. no. 9048-46-8; Amresco, Solon, OH). Subsequently, the sections were incubated with anti-MAP1LC3-A/B (cat. no. 4108S; Cell Signaling Technology, Danvers, MA), anti-CD4 (cat. no. 550280; BD Biosciences, San Jose, CA), anti-CD8 (cat. no. ab22378; Abcam, Cambridge, MA), and anti-α-smooth muscle actin (SMA) antibodies (cat. no. CBL171; Millipore, Billerica, MA) overnight at 4°C. The sections were rinsed with phosphate-buffered saline with Tween 20 (PBST) and incubated with Cy3-labeled secondary antibodies (cat. no. A0516; Beyotime), Alexa 488-conjugated antibodies (cat. no. A0428; Beyotime), and 4′,6-diamidino-2-phenylindole (DAPI; cat. no. C1002; Beyotime). The sections were observed using fluorescence microscopy (TCS SP5; Leica Microsystems, Wetzlar, Germany). For in vitro analysis, the cells were fixed with 4% paraformaldehyde followed by permeability with 0.1% Triton X-100 and blocked with 5% BSA. The cells were incubated with anti-MAP1LC3-A/B antibodies overnight at 4°C. Cells were incubated with Cy3-labeled secondary antibodies (cat. no. A0516; Beyotime) and DAPI (cat. no. C1002; Beyotime) followed by PBST washes. The slides were examined under a fluorescence microscope, and images were obtained.

2.8 | Western blot analysis

Total protein from 100 mg mouse liver tissues and MSCs subjected to the above-mentioned treatments was obtained using RIPA lysis buffer with the protein inhibitor phenylmethylsulfonyl fluoride (cat. no. ST506; Beyotime). The total protein was quantified using a BCA quantification kit (cat. no. P0010; Beyotime). Proteins were

separated using sodium dodecyl sulfate-polyacrylamide gel electrophoresis. The proteins in gel were shifted to PVDF membranes (cat. no. ISEQ. 00005; Millipore) for 90 min. Membranes were incubated with 5% milk blocking solution for 60 min and then with primary antibodies against MAP1LC3-A/B (cat. no. 4108S; Cell Signaling Technology), GAPDH (cat. no. 60004-1; Proteintech, Wuhan, China), BECN1 (cat. no. 3738S; Cell Signaling Technology), PTGS2 (cat. no. SC-166475; Santa Cruz Biotechnology, Santa Cruz, CA), p62 (cat. no. 88588; Cell Signaling Technology), and α-SMA (cat. no. CBL171; Millipore) overnight at 4°C. Membranes were then thoroughly rinsed by TBS-T and subjected to incubation of peroxidase-labeled secondary antibodies (cat. no. SA00001-1; Proteintech) for 1 hr at room temperature. The membranes were rinsed by TBS-T and then incubated with chemiluminescent HRP substrate (cat. no. WBKLSO100; Millipore). Proteins were detected with a chemiluminescence apparatus (Bio-Rad, Hercules, CA).

2.9 | Measurement of liver hydroxyproline content

Following the manufacturer's instructions, liver hydroxyproline levels were quantified by hydroxyproline detection kit (Nanjing JanCheng Biochemical Institute, Nanjing, China).

2.10 | Measurement of serum aspartate aminotransferase (AST) and alanine aminotransferase (ALT) levels

Serum concentrations of AST and ALT were detected to estimate the degree of hepatic injury caused by CCl_4 administration. Mice were anesthetized as described above, and 0.5 ml blood was obtained from the eye sockets of mice, followed by 10 min of centrifugation at 3,000 rpm. Based on the provided protocol, serum levels of AST and ALT were assessed by diagnostic quantification kits (cat. nos. C010-2 and C009-2; Nanjing JianCheng Bioengineering Institute, Nanjing, China).

2.11 | Coculture of MSCs and HSCs

MSCs and HSCs were cocultured in a Transwell coculture system (12-mm diameter; 0.4-mm pore size, cat. no. G3401; Corning, Corning, NY) with DMEM-low glucose containing 10% FBS. Briefly, HSCs at a density of 5×10^4 cells/well were cultivated in the bottom chambers of 24-well plates, and MSCs at a density of 2.5×10^3 cells/well were seeded on the Transwell membrane inserts. Three groups were evaluated, that is, control, HSCs + shNC-MSC, and HSCs + sh$Becn1$-MSC groups, with four wells per group. The HSCs were collected for analysis of proliferation and procollagen type I α1 secretion after coculturing for 24, 48, and 72 hr.

2.12 | Enzyme-linked immunosorbent assay (ELISA)

After coculture with MSCs for 72 hr, HSCs were collected, and supernatants were obtained to determine secretion of procollagen type I α I (cat. no. ab210579; Abcam) using an ELISA kit. The

absorbance (OD value) was measured at 450 nm. shNC-MSCs and sh$Becn1$-MSCs were incubated with TNF-α (20 ng/ml), IFN-γ (50 ng/ml), and TGF-β1 (10 ng/ml) alone or in combination for 24 hr. Supernatants were then obtained to detect prostaglandin E_2 (PGE$_2$) secretion using a PGE$_2$ ELISA kit (cat. no. KGE004B; R&D Systems). For in vivo experiments, the levels of serum PGE$_2$, TNF-α, TGF-β1, and IFN-γ were determined using PGE$_2$, TNF-α (cat. no. KE10002; Proteintech), IFN-γ (cat. no. KE10001; Proteintech), and TGF-β1 (cat. no. KE10005; Proteintech) ELISA kits.

2.13 | Real-time PCR

Total RNA of MSCs was extracted at the indicated time points with TRIzol Reagent (Invitrogen, Carlsbad, CA). Synthesis of complementary DNA (cDNA) from mRNA was performed via reverse transcription with an iScript cDNA synthesis kit (cat. no. 170-8890; Bio-Rad). qPCR was conducted in triplicate using SYBR Green Supermix (cat. no. 172-5271; Bio-Rad). GAPDH was utilized an internal control. The primer sequences are listed in Table 1.

2.14 | Statistical analysis

All data are expressed as means ± *SEM*s, and were statistically analyzed using GraphPad Prism 5 (GraphPad Software Inc., La Jolla, CA). Means of two groups were compared by Student's *t* tests. For multiple comparisons, statistical analysis was performed by analysis of variance. A $p < .05$ was considered statistically significant.

3 | RESULTS

3.1 | Autophagy of MSCs occurred in a LF microenvironment

To determine whether autophagy of MSCs occurred during LF, EGFP-control lentivirus-transfected MSCs (shNC-MSCs) were transfused into oil mice or CCl_4 mice via the tail vein. Interestingly, the number of EGFP$^+$ MSCs and the extent of MAP1LC3 puncta in the

TABLE 1 Primer pairs used for PCR

Gene	Sequence
GAPDH	Fw 5′-AGGTCGGTGTGAACGGATTTG-3′
	Rv 5′-TGTAGACCATGTAGTTGAGGTCA-3′
TNF-α	Fw 5′-CTATGGCCCAGACCCTCACA-3′
	Rv 5′-TTGAGATCCATGCCGTTGGC-3′
IFN-γ	Fw 5′-GCGCCAAGCATTCAATGAGC-3′
	Rv 5′-CAGCGACTCCTTTTCCGCTT-3′
TGF-β1	Fw 5′-TTCAGCGCTCACTGCTCTTG-3′
	Rv 5′-TTGGTATCCAGGGCTCTCCG-3′
Becn1	Fw 5′-AGGCGAAACCAGGAGAGAC-3′
	Rv 5′-CCTCCCCGATCAGAGTGAA-3′

Abbreviations: Fw, forward primer; PCR, polymerase chain reaction; Rv, reverse primer.

MSCs were increased in CCl4 mice, but not in oil mice at 72 hr following cell administration (Figure 1a).

MSCs were cultivated with or without TNF-α, IFN-γ, and TGF-β1, and autophagy activation in MSCs was analyzed. Cells that underwent starvation served as positive controls. Significant increases in the MAP1LC3-II/MAP1LC3-I ratio were observed in MSCs stimulated with TNF-α, IFN-γ, or TGF-β1 for different time points, with the most obvious elevation occurring at 6 hr (Figure 1b). Furthermore, we found that among the three LF-related cytokines, IFN-γ treatment induced marked elevation in autophagosome formation in MSCs, as observed by transmission electron microscopy (Figure 1c) and fluorescence microscopy (Figure 1d,e).
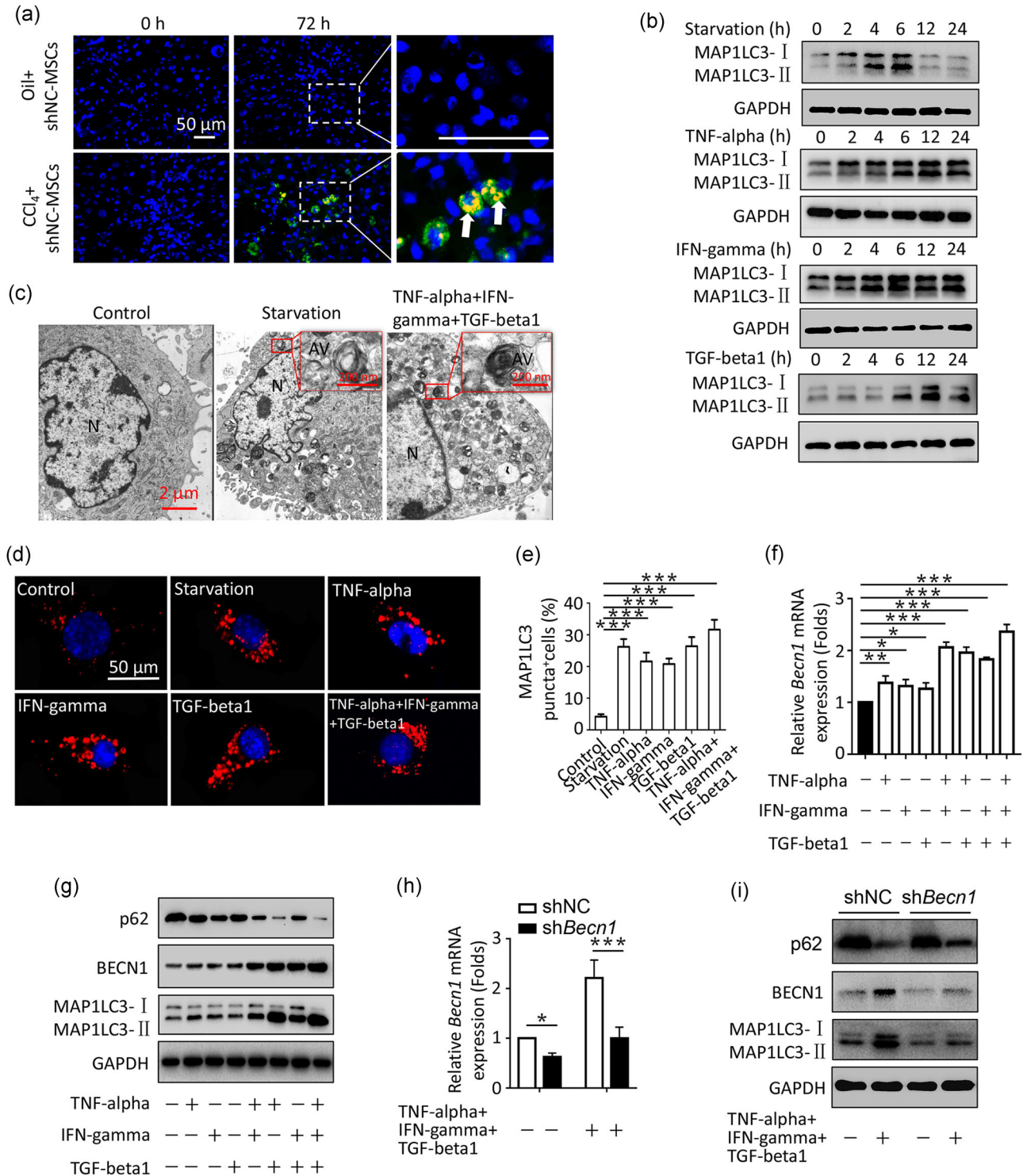

FIGURE 1 Continued.

3.2 | LF-related cytokines triggered autophagy in MSCs via upregulation of BECN1

To determine whether the autophagy activated by LF-related cytokines was triggered by upregulating BECN1, MSCs were stimulated with the three cytokines alone or in different combinations for 6 hr. All treatments significantly upregulated mRNA and protein expression of BECN1 (Figure 1f,g) downregulated p62 protein expression (Figure 1g).

To further explore the function that BECN1 played in autophagy, lentivirus-expressing shRNA specific to *Becn1* (sh*Becn1*-MSCs) was used to downregulate BECN1 expression in MSCs. Subsequently, the cells were cultivated with or without TNF-α, IFN-γ, and TGF-β1. For the control group, MSCs were transfected with a lentivirus-expressing scrambled shRNA (shNC-MSCs). We revealed that *Becn1* knockdown reduced the MAP1LC3-II/MAP1LC3-I ratio and increased p62 expression levels after treatment with or without the three LF-related cytokines compared with that in the control shRNA-MSCs (Figure 1h,i). These findings suggested that treatment with the three LF-related cytokines triggered autophagy in MSCs by upregulation of BECN1.

3.3 | Knockdown of *Becn1* promoted the antifibrotic efficacy of MSCs in CCl₄-induced LF

To explore whether autophagy inhibition by *Becn1* knockdown affected the therapeutic capacity of MSCs in LF, shNC-MSCs and sh*Becn1*-MSCs were injected weekly into mice via the tail vein from Weeks 3 to 5. After 5 weeks, the extent of LF was evaluated via histopathological analyses. Gross examination showed that livers of mice in the CCl₄ + sh*Becn1* group were smoother and softer than those of mice in the CCl₄ + PBS and CCl₄ + shNC groups. The hepatic pathological changes were significantly ameliorated in the sh*Becn1*-MSC-treated group in contrast to those in the CCl₄ + PBS and CCl₄ + shNC groups (Figure 2a). Moreover, HE, Masson, and Sirius red staining all indicated that transplantation of sh*Becn1*-MSCs markedly ameliorated LF, as indicated by reduced collagen deposition, smaller fibrotic areas, and decreased inflammatory cell infiltration as compared to those observed in the CCl₄ + PBS and CCl₄ + shNC groups (Figure 2a).

α-SMA is a biomarker of myofibroblasts, and hydroxyproline levels in liver reflect the severity of LF. Therefore, α-SMA expression and hydroxyproline levels in liver were detected, and the results indicated that administration of sh*Becn1*-MSCs reduced α-SMA expression and hydroxyproline levels in fibrotic livers as compared with those in CCl₄ + PBS and CCl₄ + shNC groups (Figure 2b,c). Furthermore, reduced AST and ALT levels were observed in fibrotic livers of mice treated with sh*Becn1*-MSCs compared with those in mice in the CCl₄ + PBS and CCl₄ + shNC groups (Figure 2d). Taken together, these results confirmed that autophagy inhibition primed by *Becn1* stable knockdown in MSCs could increase their antifibrotic efficacy in LF.

3.4 | sh*Becn1*-MSCs inhibited HSCs and Gli1⁺ cell proliferation and decreased procollagen I α1 secretion in HSCs

HSCs activation and proliferation are essential in the hepatic response to injury and liver fibrogenesis. In this study, an in vitro coculture system of HSCs and MSCs was used to further verify the mechanisms through which sh*Becn1*-MSCs ameliorate LF. The effects of shNC-MSCs and sh*Becn1*-MSCs on HSCs proliferation were evaluated following a coculture of 24, 48, and 72 hr. Significant decreases in the numbers of HSCs were noted 48 and 72 hr after coculture (Figure 3a). Furthermore, analysis of the effects of shNC-MSCs and sh*Becn1*-MSCs on procollagen I α1 secretion from HSCs showed that there was a significant decrease in procollagen I α1 secretion in the sh*Becn1*-MSC group after 72 hr of coculture compared with that in the control and shNC-MSC groups (Figure 3b). Because HSCs are the predominant origin of myofibroblasts progenitors and *Gli1* is an in vivo marker of myofibroblast progenitors (Kramann et al., 2015), *Gli1* genetic lineage-tracing mice were utilized to detect the impact of sh*Becn1*-MSCs on Gli1⁺ cells in the fibrotic liver in vivo. Our results showed that Gli1⁺ cells in fibrotic

FIGURE 1 Autophagy of mesenchymal stem cells (MSCs) occurred under liver fibrosis microenvironment. (a) MSCs were transfused into oil mice and CCl₄ mice via tail vein at 5 weeks following oil or CCl₄ administration. Mice were euthanized at 0 and 72 hr after cell administration, and livers were cut into frozen sections. Sections were incubated with anti-MAP1LC3-A/B antibodies and DAPI and visualized under a fluorescent microscope. (b) Western blot analysis of MAP1LC3-I/MAP1LC3-II expression in MSCs starved or stimulated with tumor necrosis factor-α (TNF-α), interferon-γ (IFN-γ), or transforming growth factor-β1 (TGF-β1) for 0–24 hr. The blots shown are representative of three independent experiments. (c) The MSCs were starved, not starved (control), or stimulated with TNF-α, IFN-γ, and TGF-β1 for 6 hr. Autophagosomes in MSCs were visualized using transmission electron microscopy. Representative images of three independent experiments are presented. AV, autophagic vacuoles; N, nucleus. (d, e) Immunofluorescence staining of MAP1LC3 in MSCs starved, not starved (control), or primed with TNF-α, IFN-γ, and TGF-β1 alone or in varied combinations for 6 hr. The representative images from three independent experiments are shown. The MSCs presented with MAP1LC3 dots were numbered for five images from each group. (f) *Becn1* messenger RNA (mRNA) expression in MSCs stimulated without or with TNF-α, IFN-γ, or TGF-β1 alone or in varied combinations were detected using quantitative polymerase chain reaction (qPCR). (g) Western blot analysis showing MAP1LC3-I, MAP1LC3-II, and p62 expression in MSCs stimulated with TNF-α, IFN-γ, and TGF-β1 alone or in varied synergies for 6 hr. Representative data from three experiments are shown. (h) shNC-MSCs and sh*Becn1*-MSCs were cultivated in absence or presence of TNF-α, IFN-γ, and TGF-β1. *Becn1* mRNA expression was measured using qPCR. (i) The protein expression levels of MAP1LC3-I, MAP1LC3-II, BECN1, and p62 were detected using western blot analysis. Data are presented as means ± *SEM*s. *$p < .05$, **$p < .01$, ***$p < .001$. In all cases the concentrations used for treatments were as follows: TNF-α (20 ng/ml), IFN-γ (50 ng/ml), and TGF-β1 (10 ng/ml). DAPI, 4′,6-diamidino-2-phenylindole
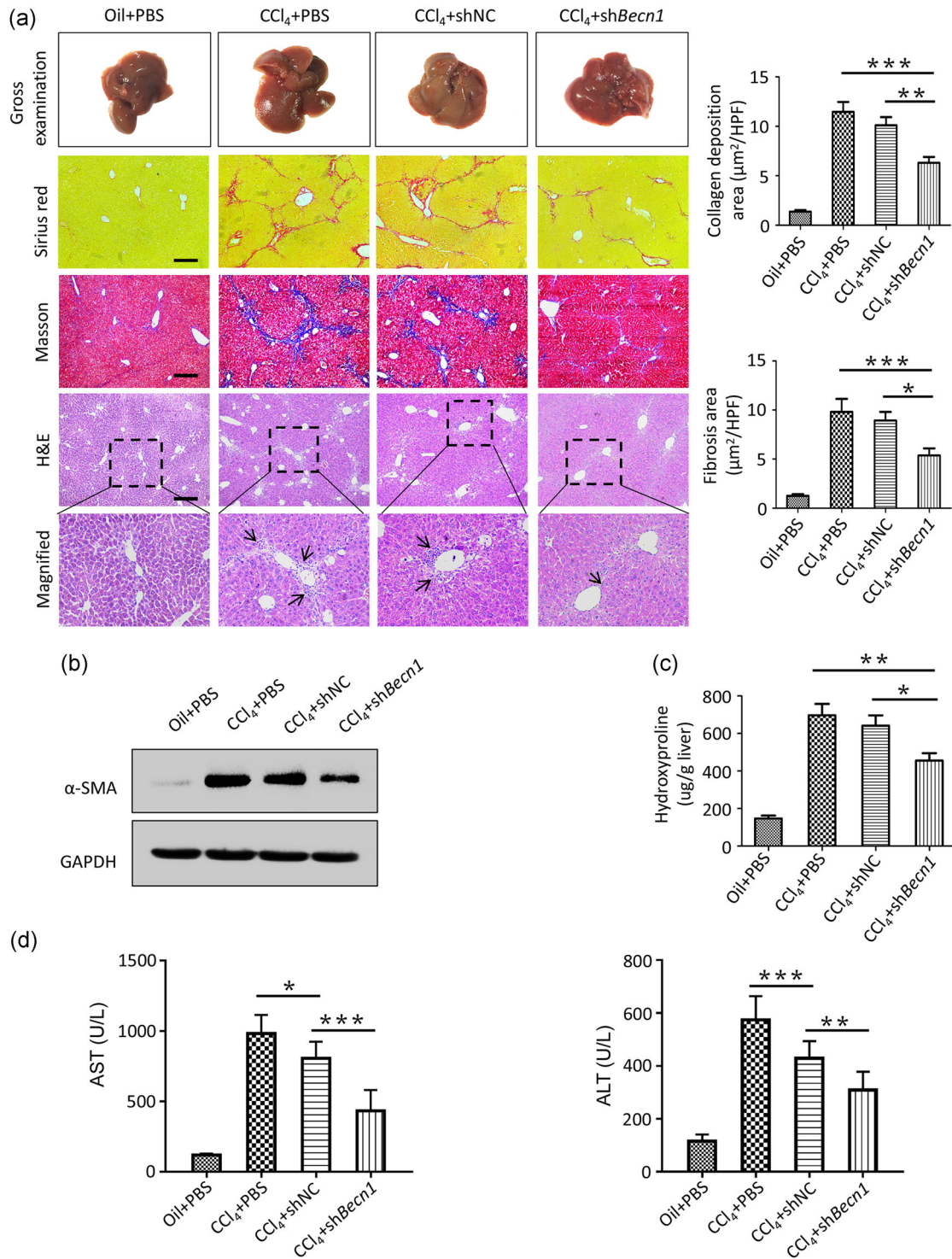
FIGURE 2 *Becn1* knockdown promoted the antifibrotic efficacy of mesenchymal stem cells in CCl_4-induced liver fibrosis. (a) Mice were randomly selected and designated as the oil + PBS, CCl_4 + PBS, CCl_4 + shNC, and CCl_4 + sh*Becn1* groups (n = 8). Mice were euthanized 3 days after cell transplantation, and pathological alterations in the liver were detected by gross examination, Sirius red staining, Masson staining, and HE staining. Quantification of fibrosis was analyzed, and representative microscopy images are presented. (b) Western blot analysis of α-SMA in livers subjected to the indicated treatments. (c) The levels of hydroxyproline were detected in livers subjected to different treatments. (d) Serum concentrations of AST and ALT were determined to indicate the extent of liver parenchyma damage caused by CCl_4 administration. Scale bar, 200 μm. The results are presented as means ± *SEM*s. ALT, alanine aminotransferase; AST, aspartate aminotransferase; HE, hematoxylin and eosin; PBS, phosphate-buffered saline; α-SMA, α-smooth muscle actin. *p < .05, **p < .01, ***p < .001
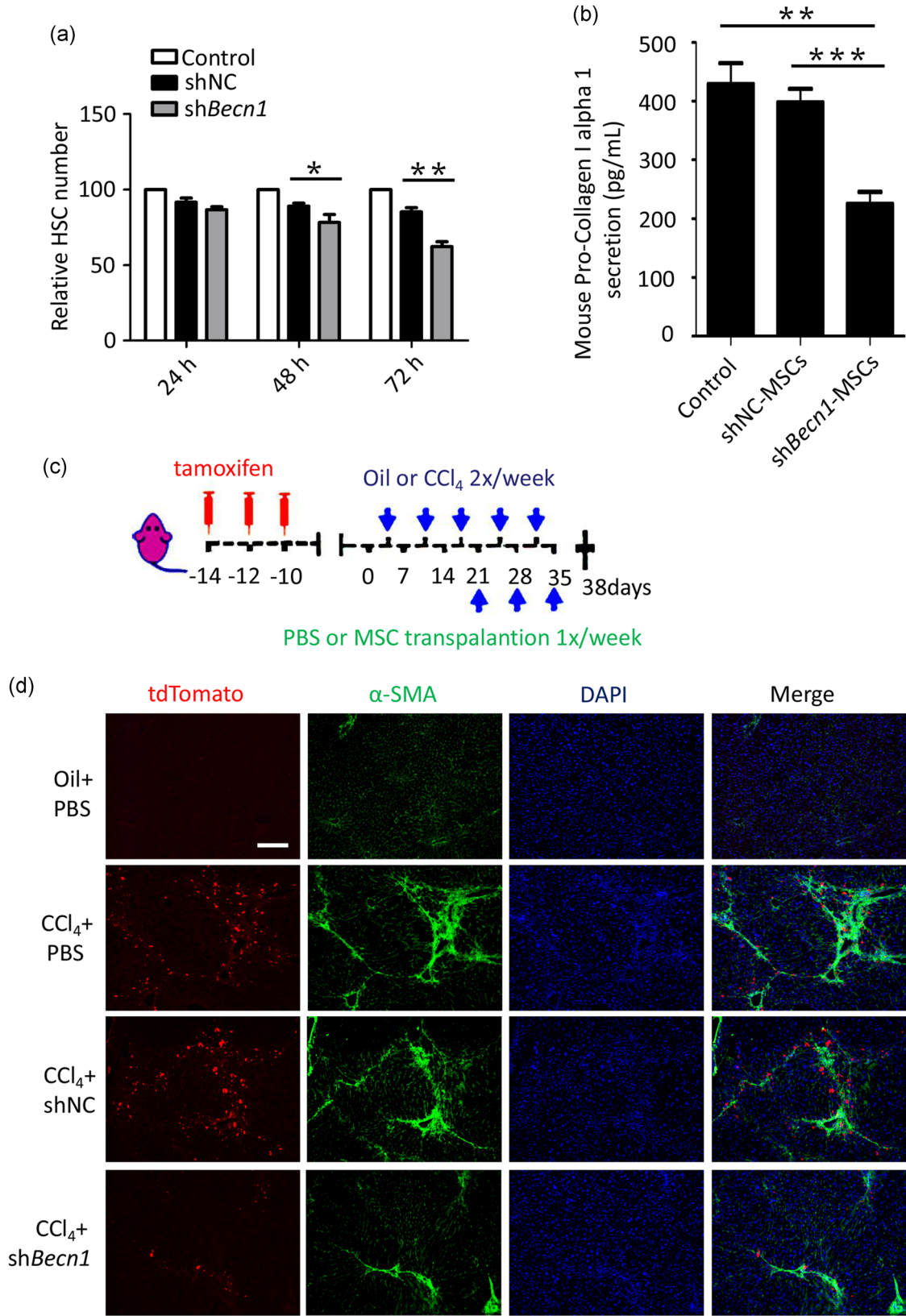
FIGURE 3   Continued.

livers were significantly reduced after transplantation of sh*Becn1*-MSCs (Figure 3c,d). These results unveiled that the promoted antifibrotic capability of sh*Becn1*-MSCs in LF might be attributed to their inhibitory effects on HSCs proliferation.

3.5 | sh*Becn1*-MSCs attenuated infiltration of CD4^{+} and CD8^{+} T lymphocytes in CCl$_4$-induced fibrotic livers

The involvement of CD4^{+} and CD8^{+} T lymphocyte infiltration in LF has been confirmed (Pesce et al., 2006; Wynn, 2004). Therefore, changes in T lymphocyte populations in the liver upon MSC treatment were further investigated to determine the mechanisms through which sh*Becn1*-MSCs alleviated LF. Fluorescence microscopy results demonstrated that the numbers of CD4^{+} and CD8^{+} T lymphocytes were increased in CCl$_4$-induced fibrotic livers. Notably, sh*Becn1*-MSCs substantially lowered the numbers of CD4^{+} and CD8^{+} T cells infiltrating the CCl$_4$-induced fibrotic livers compared with that in the shNC-MSC group (Figure 4a,b). Indeed, our findings showed that BECN1 downregulation in MSCs triggered a decrease in the absolute numbers of CD4^{+} and CD8^{+} lymphocytes in CCl$_4$-induced fibrotic livers. Thus, these observations suggested that autophagy suppression in MSCs modulated by *Becn1* stable knockdown could suppress T-cell infiltration in the fibrotic liver, indicating that the decreased CD4^{+} and CD8^{+} T-cell infiltration accounted for the strengthened antifibrotic effects of sh*Becn1*-MSCs in CCl$_4$-induced LF mice.

3.6 | Chemotaxis of exogenous MSCs into fibrotic livers and colocalization of exogenous MSCs, Gli1^{+} cells, and T cells in LF

shNC-MSCs and sh*Becn1*-MSCs were administered into oil or CCl$_4$ mice, and the localization of MSCs was detected at 3 days after cell transplantation under a fluorescence microscope. Notably, transplanted shNC-MSCs and sh*Becn1*-MSCs were recruited to CCl$_4$-induced fibrotic livers, as demonstrated by significant increases in the numbers of EGFP^{+} cells located in CCl$_4$-induced fibrotic livers; few EGFP^{+} cells were found in normal livers (Figure 5a). In addition, immunofluorescence staining for α-SMA demonstrated the colocalization of exogenous MSCs and fiber collagen accumulation in fibrotic livers (Figure 5b).

Immunofluorescence staining was then conducted for evaluating the distributions of CD4^{+} and CD8^{+} T lymphocytes in CCl$_4$-induced fibrotic livers. In addition, *Gli1*-CreERt2;*tdTomato* genetic lineage-tracing mice were utilized to assess the distribution of Gli1^{+} cells in CCl$_4$-induced fibrotic livers. Notably, immunofluorescence staining demonstrated that CD4^{+} and CD8^{+} T cells and Gli1^{+} cells were all mainly deposited in the α-SMA^{+} portal area, suggesting the colocalization of the three cell types within the fibrotic portal area in CCl$_4$-induced fibrotic livers (Figure 5c,d). These findings provided direct evidence for colocalization of the transplanted MSCs, Gli1^{+} cells, and CD4^{+} and CD8^{+} T lymphocytes in the portal fibrotic area in CCl$_4$-induced fibrotic livers.

3.7 | Knockdown of *Becn1* suppressed autophagy and promoted the expression of PTGS2/PGE$_2$ in MSCs

Next, we explored the mechanisms delineating the increased antifibrotic efficacy of sh*Becn1*-MSCs in fibrotic livers. shNC-MSCs and sh*Becn1*-MSCs were administered intravenously into CCl$_4$ mice, and autophagy activity of MSCs was detected. A significant decrease in MAP1LC3 dot formation was observed in sh*Becn1*-MSCs compared with that in shNC-MSCs (Figure 6a). We confirmed that the liver fibrotic microenvironment induced autophagy in MSCs. Therefore, the impact of *Becn1* knockdown on autophagic activity in MSCs was determined. MSCs were treated with inflammatory cytokines in presence or absence of the classical autophagy inhibitor 3-MA or the well-characterized autophagy inducer rapamycin, and MAP1LC3-I, MAP1LC3-II, and p62 expression levels were assayed. In the sh*Becn1*-MSC group treated with the three LF-related cytokines, reduced MAP1LC3-II/MAP1LC3-I ratios, but elevated PTGS2 expression were observed compared with those in the shNC-MSC group; however, rapamycin treatment abrogated the effects of sh*Becn1*-MSCs (Figure 6b). Similarly, 3-MA treatment decreased the MAP1LC3-II/MAP1LC3-I ratio and upregulated p62 expression in shNC-MSCs treated with the three LF-related cytokines (Figure 6b). In addition, secretion of PGE$_2$, a downstream product of PTGS2 and an effector of immunosuppression, in MSCs treated with the three LF-related cytokines was markedly elevated in the supernatant fraction of sh*Becn1*-MSCs compared with that of shNC-MSCs (Figure 6c). The elevation of PGE$_2$ was also observed in the sera of sh*Becn1*-MSC-treated mice with LF compared with that in mice treated with

FIGURE 3 sh*Becn1*-MSCs inhibited HSCs and Gli1^{+} cell proliferation and decreased procollagen I α1 secretion in HSCs. (a) Effects of MSCs on HSCs proliferation were examined using CCK-8 assays in the coculture system with PBS, shNC-MSCs, or sh*Becn1*-MSCs for the indicated times. (b) After coculturing with PBS, shNC-MSCs, or sh*Becn1*-MSCs for 72 hr, HSCs were collected for detection of procollagen type I α1 secretion using enzyme-linked immunosorbent assay (*n* = 4). (c) To trace *Gli1*^{+} cells in vivo, *Gli1*-CreERt2;*tdTomato* genetic lineage-tracing mice underwent three intraperitoneal injections of tamoxifen (3 × 0.1 mg/kg) every other day at 14 days before LF induction. Mice LF model was established via intraperitoneal injection of CCl$_4$ olive oil solution (CCl$_4$:olive oil = 1:3) twice per week for 5 consecutive weeks. MSCs or PBS were administered into mice weekly from Weeks 3 to 5 via the tail vein. (d) Mice were divided into the oil + PBS, CCl$_4$ + PBS, CCl$_4$ + shNC, and CCl$_4$ + sh*Becn1* groups (*n* = 8) and were euthanized 3 days after cell administration. Frozen sections of the liver was stained with anti-α-SMA antibodies and counterstained with DAPI. The observation of tdTomato expression was carried out under a fluorescent microscope. Scale bar, 200 μm. Data are presented as means ± *SEM*s. HSCs, hepatic stellate cells; LF, liver fibrosis; MSCs, mesenchymal stem cell; PBS, phosphate-buffered saline; α-SMA, α-smooth muscle actin. *p < .05, **p < .01, ***p < .001
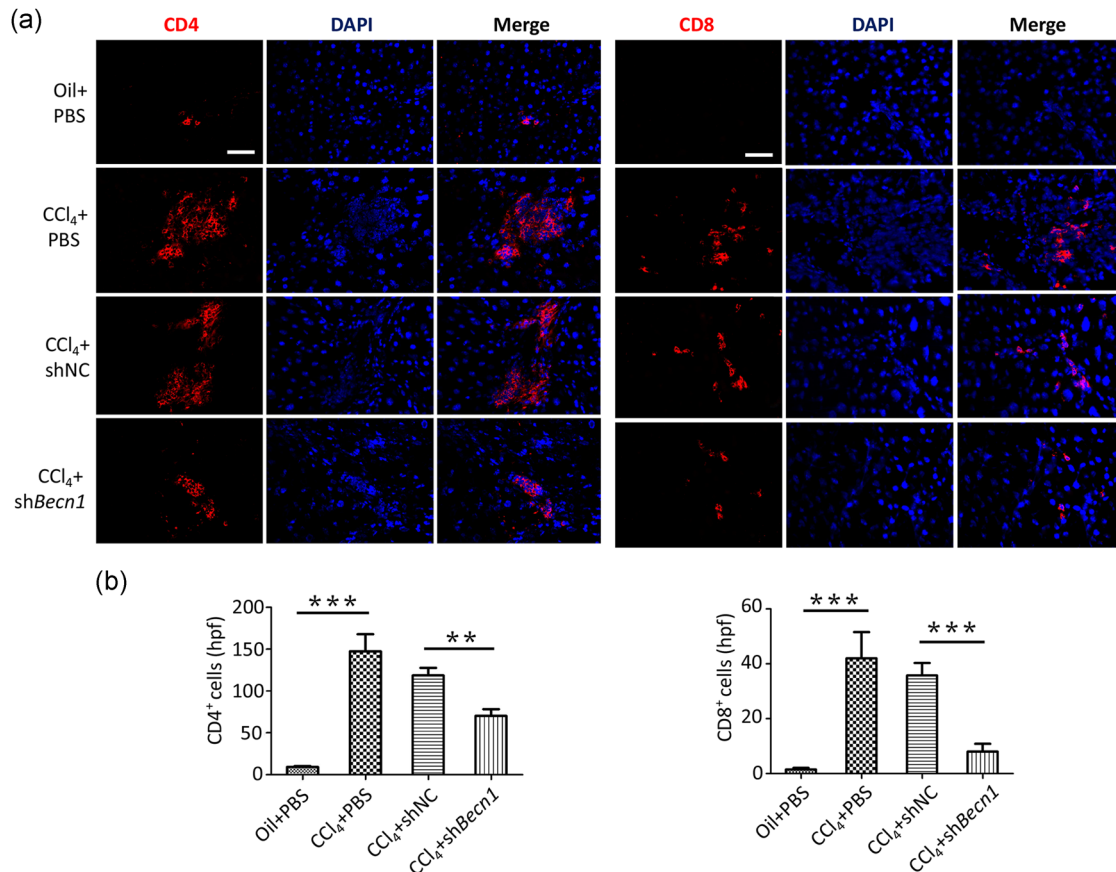
FIGURE 4 Accumulation of CD4$^+$ and CD8$^+$ lymphocytes in fibrotic livers was substantially attenuated in sh*Becn1*-MSC-treated CCl$_4$ mice. (a) Mice were euthanized 3 days after cell transplantation. Livers were resected from oil mice and CCl$_4$ mice treated with PBS, shNC-MSC, or sh*Becn1*-MSC followed by OCT embedding. Frozen sections were incubated with CD4 and CD8 primary antibodies and observed under a fluorescent microscope. Representative figures are presented. Scale bars, 50 μm. (b) Quantitative analysis of CD4$^+$ and CD8$^+$ lymphocytes numbers was performed in a ×400 hpf. The findings are expressed as means ± *SEM*s. MSC, mesenchymal stem cell; PBS, phosphate-buffered saline. **$p < .01$, ***$p < .001$

shNC-MSCs or PBS (Figure 6d). The mRNA expression levels of key LF-related cytokines were markedly decreased in LF and in the sera of sh*Becn1*-MSC-treated mice with LF as compared with those in mice treated with shNC-MSCs (Figure 6e,f). These results indicated that sh*Becn1*-MSCs potentiated the antifibrotic efficacy of MSCs by suppressing inflammation-induced autophagy and generating more PGE$_2$.

4 | DISCUSSION

Although the potent immunosuppressive function of MSCs renders them attractive candidates for antifibrotic treatments, the consequent responses of MSCs under hepatic context following transplantation needs to be further elucidated, as their therapeutic efficacy is inconsistent (Alfaifi, Eom, Newsome, & Baik, 2018; Consentius, Reinke, & Volk, 2015). The inconsistent findings gained from different studies are attributable to the different sources and lack of control over the cell fate of the transplanted MSCs in vivo. Therefore, determining mechanisms through which the LF

microenvironment controls the immunoregulatory functions of MSCs and the fate of MSCs is expected to deliver new insights into improving the efficacy of MSC-based immunotherapy.

In this study, we revealed that autophagy occurred in MSCs due to reaction with the LF microenvironment. Indeed, the LF microenvironment suppressed the treatment efficacy of the transplanted MSCs via autophagy induction. Nevertheless, counteracting LF microenvironment-induced autophagy by *Becn1* knockdown significantly promoted the antifibrotic effects of MSCs. The improved antifibrotic potential of sh*Becn1*-MSCs may be attributable to their improved suppression of CD4$^+$ and CD8$^+$ T lymphocyte accumulation and HSCs and Gli1$^+$ cell proliferation. Furthermore, we found that *Becn1* knockdown in MSCs altered PTGS2/PGE$_2$ secretion, resulting in potent immunoregulatory effects. These findings suggested that autophagy regulation in MSCs might serve as a promising remedy to improve the antifibrotic efficacy of MSCs on LF and other inflammatory disorders.

Recent studies have shown that the results of MSC-based therapies are determined by the interplay between MSCs and the inflammatory microenvironment (Mougiakakos et al., 2011; Ren
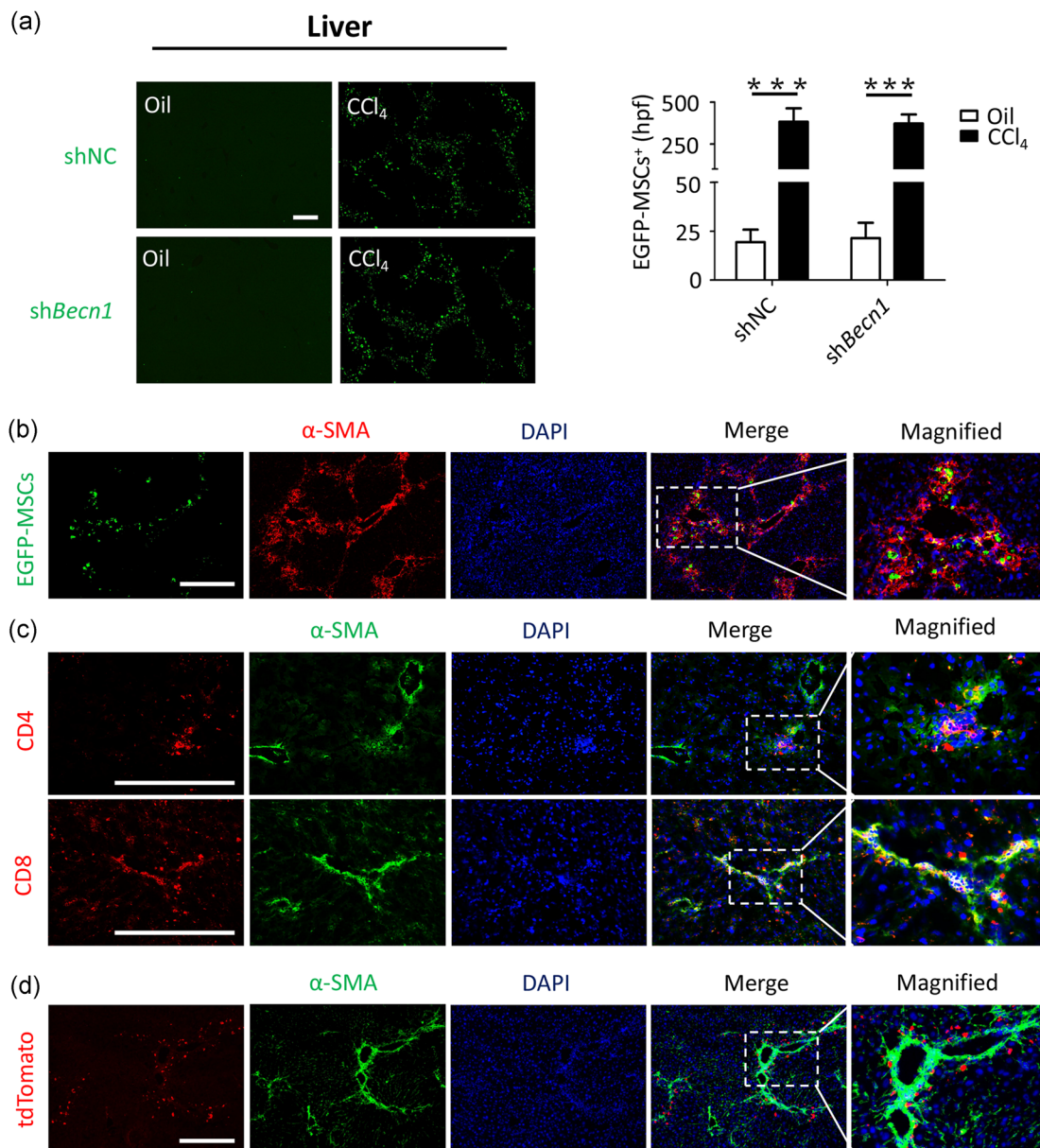
FIGURE 5 Chemotaxis of exogenous mesenchymal stem cell (MSCs) into fibrotic livers and colocalization of exogenous MSCs, T cells, and Gli1^{+} cells in liver fibrosis (LF). (a) Oil and CCl$_4$ mice treated with shNC-MSCs or sh*Becn1*-MSCs (on Week 5) were killed 3 days after cell transplantation. MSCs in the liver were visualized under a fluorescent microscope. The numbers of MSCs in the liver were measured in ×50 hpf. Representative images are presented. The findings are expressed as means ± *SEM*s. ***p < .001. (b) CCl$_4$ mice were treated with shNC-MSCs and killed 3 days after cell transplantation. Liver sections from these mice were incubated with anti-α-SMA antibodies, and sections were visualized under a fluorescent microscope. Representative images are shown. (c) CCl$_4$ mice were killed, and frozen sections of liver sections were incubated with CD4, CD8, and α-SMA primary antibodies. CD4^{+} and CD8^{+} lymphocytes and α-SMA^{+} cells were visualized under a fluorescent microscope. (d) The LF model was built by CCl$_4$ injection using *Gli1*-CreERt2;td*Tomato* genetic lineage-tracing mice. Liver sections were incubated with anti-α-SMA antibody. The α-SMA[+] and Gli1^{+} cells were examined using fluorescent microscopy. Scale bars, 500 μm. α-SMA, α-smooth muscle actin

et al., 2008). For example, studies performed by Shi et al. (2010) indicated that TNF-α and IFN-γ are critical cytokines inducing immunosuppression of MSCs. Interleukin (IL)-17 cooperates with IFN-γ and TNF-α to evoke immunoinhibition via boosting expression of inducible nitric oxide synthase in MSCs (Han et al., 2014). In the current study, shNC-MSCs were transfused into oil mice and CCl$_4$ mice. Notably, we confirmed that MSCs exhibited autophagy under

the context of LF microenvironment in vivo, as demonstrated by marked increases in EGFP[+] MSCs and MAP1LC3 puncta in the MSCs in CCl$_4$ mice.

Proinflammatory cytokines, such as TNF-α and IFN-γ, have vital effect on pathogenesis of LF (Seki & Schwabe, 2015). TGF-β1 is a master profibrotic factor and regulator of LF, and blocking TGF-β1 signaling pathways decreases fibrogenesis in animal models (Meng,
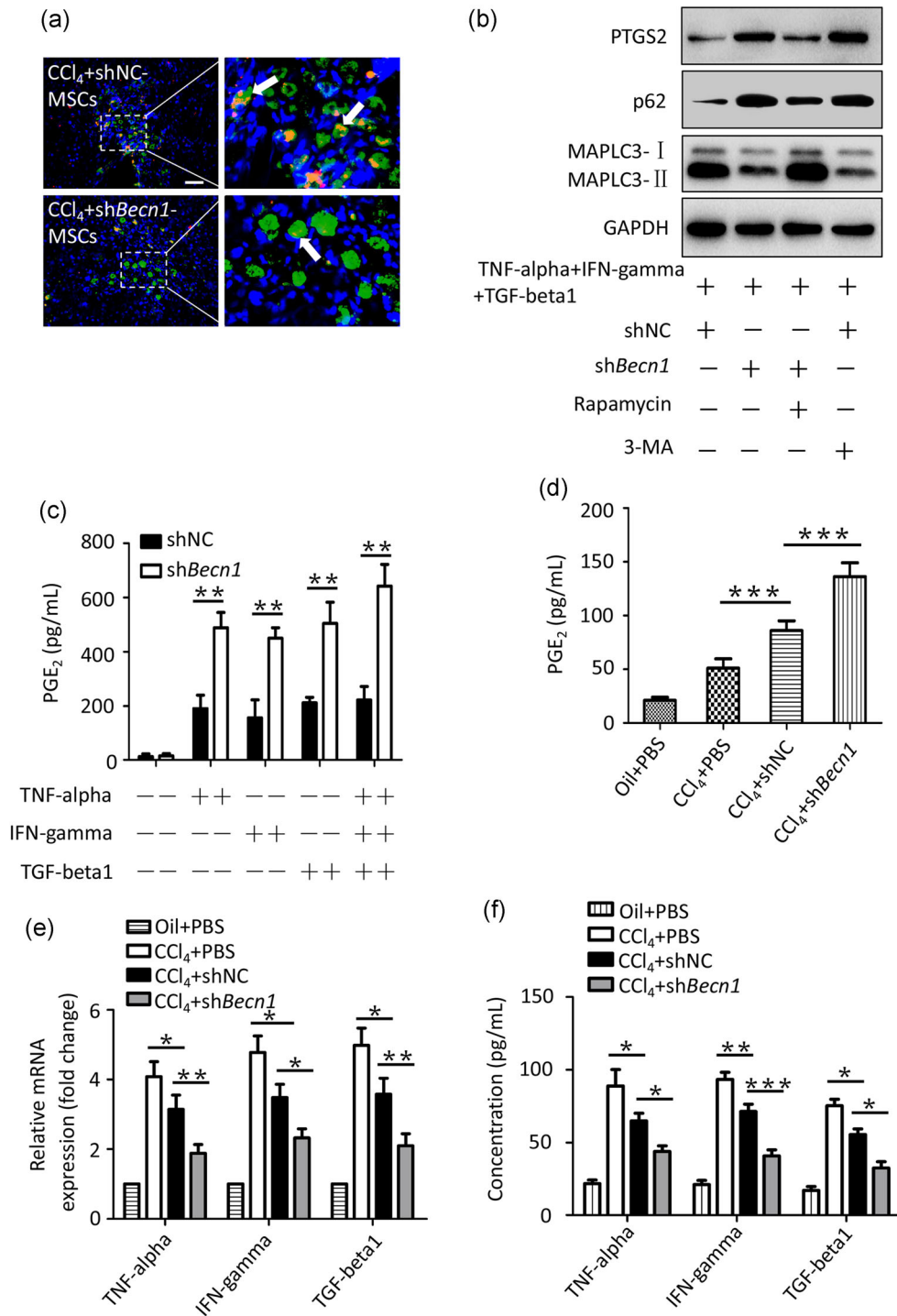
FIGURE 6 Knockdown of *Becn1* suppressed inflammation-induced autophagy and generated more PTGS2/PGE$_2$ in mesenchymal stem cells (MSCs). (a) shNC-MSCs and sh*Becn1*-MSCs were injected into liver fibrosis model mice, which were euthanized 3 days posterior to cell infusion. Frozen sections of liver tissues were stained with anti-MAP1LC3-A/B antibodies with nuclei counterstained with DAPI and visualized under a fluorescent microscopy. (b) The expression levels of PTGS2, p62, MAP1LC3-I, and MAP1LC3-II in MSCs were determined by western blot analysis analysis. shNC-MSCs were incubated in presence or absence of 3-MA, and sh*Becn1*-MSCs were incubated in presence or absence of rapamycin, under combined stimulation with tumor necrosis factor-α (TNF-α, 20 ng/ml), interferon-γ (IFN-γ, 50 ng/ml), and transforming growth factor-β1 (TGF-β1, 10 ng/ml) for 12 hr. (c) shNC-MSCs and sh*Becn1*-MSCs underwent single or combined treatment with TNF-α (20 ng/ml), IFN-γ (50 ng/ml), or TGF-β1 (10 ng/ml) for 24 hr, and PGE$_2$ secretion in the supernatant was assayed using enzyme-linked immunosorbent assay (ELISA). The results are presented as means ± *SEM*s. (d) Mice were divided into the oil + PBS, CCl$_4$ + PBS, CCl$_4$ + shNC, and CCl$_4$ + sh*Becn1* groups and euthanized. Subsequently, serum levels of PGE$_2$ were quantified using ELISA, and (e) *TNF-α, IFN-γ*, and *TGF-β1* messenger RNA expression in the mice liver were measured by quantitative polymerase chain reaction. (f) Serum concentrations of TNF-α, IFN-γ, and TGF-β1 were determined using ELISA. The findings are expressed as means ± *SEM*s. PGE$_2$, prostaglandin E$_2$; PTGS2, prostaglandin-endoperoxide synthase 2. *p < .05, **p < .01, ***p < .001

Nikolic-Paterson, & Lan, 2016). TGF-β1 induces the production and inhibits the degradation of ECM proteins. Indeed, our results confirmed that TNF-α, IFN-γ, and TGF-β1 treatment induced marked increases in autophagosome formation, accompanied by significant increases in the MAP1LC3-II/MAP1LC3-I ratio. TNF-α or IFN-γ stimulated autophagy in MSCs at about 4 hr, while TGF-β1 induced increased autophagy in MSCs later than TNF-α and IFN-γ. This may be attributed to early inflammatory factors of liver damage such as TNF-α and IFN-γ, which activate immune cells and induce inflammation (Ge, Huang, & Yao, 2018). TGF-β1 is an important profibrotic factor and an immunomodulatory molecule (Fujio et al., 2016). Due to the different effects of these factors, there may be differences in the timing of induction of autophagy in MSCs. In vitro studies in MSCs further confirmed the crosstalk between autophagy and the LF microenvironment, consistent with our *in vivo* findings and with the previous findings demonstrating that TNF-α and IFN-γ could activate autophagy in various cell types (Yuan et al., 2018). Moreover, our results were further supported by a study confirming that TGF-β1 stimulates autophagy, suggesting that autophagy may participate in fibrosis via the TGF-β1 pathway (Ghavami et al., 2015). Taken together, these findings suggested that the microenvironment of LF, as defined by chronic inflammatory responses involving the proinflammatory factors TNF-α and IFN-γ and the subsequent repair process regulated by the profibrotic factor TGF-β1, triggered autophagy in MSCs both in vivo and in vitro.

We also found that the three LF-related cytokines upregulated both the mRNA and protein expression of BECN1, and downregulated p62 protein expression in MSCs. Consistent with this, *Becn1* knockdown reduced the MAP1LC3-II/MAP1LC3-I ratio and increased P62 expression in MSCs. These findings suggested that the autophagy triggered by the three LF-related cytokines might be attributed to BECN1 upregulation in MSCs, which supported the past research demonstrating that IFN-γ and TNF-α trigger BECN1 expression to induce autophagy (Djavaheri-Mergny et al., 2006; Tu et al., 2011) and that autophagy is inhibited by reducing TGF-β1 secretion and TGF-β1/Smad signaling (T. Liu et al., 2018).

As an evolutionarily highly conserved cellular process, autophagy functions to maintain intracellular homeostasis (Cadwell, 2016). Emerging evidence has shown close crosstalk between autophagy and immunomodulation (Clarke & Simon, 2018). Moreover, autophagy plays pivotal role in T-cell homeostasis and can modulate Th1/Th2 T-cell responses (Deretic, 2012). In the present study, we revealed the promoted antifibrotic capability of sh*Becn1*-MSCs in LF in contrast to that in shNC-MSCs. Importantly, proinflammatory cytokines are a prerequisite for MSCs to exert their immune-inhibitory functions (Ren et al., 2008). Nevertheless, these cytokines may initiate a negative feedback loop to curb the immunosuppressive properties of MSCs by activating autophagy under LF microenvironment. Conversely, inhibiting autophagy by *Becn1* knockdown endowed MSCs with improved antifibrotic properties in CCl₄-induced mice, as demonstrated by decreased collagen deposition, inflammatory cell infiltration, necrotic hepatocytes, and reduced serum concentrations of AST and ALT in the sh*Becn1*-MSC group

(Dang et al., 2014) found that inflammatory condition hampered the immunoinhibitive potential of MSCs by priming autophagy in a mouse model of experimental autoimmune encephalitis, supporting our findings. Similar results indicating protective effect of bone MSCs on n-hexane-induced neuropathy through autophagy inhibition were also found in another study (Hao et al., 2018). Collectively, our results demonstrate that counteracting LF microenvironment-induced autophagy via stable knockdown of *Becn1* remarkably promotes the antifibrotic effects of MSCs.

Myofibroblasts derived from HSCs are a potential therapeutic target for antifibrotic therapies (Puche, Saiman, & Friedman, 2013). Interestingly, a genetic lineage-tracing analysis performed by Kramann et al. (2015) strongly suggested that Gli1 is a specific biomarker for myofibroblast progenitors. Our results suggested that sh*Becn1*-MSCs inhibited the proliferation of HSCs both in vivo and in vitro and decreased the secretion of procollagen I α1 in HSCs in an in vitro coculture system. These findings affirmed that the inhibitive function on HSCs proliferation might contribute to the augmented therapeutic consequence of sh*Becn1*-MSCs in LF.

The onset and progression of LF are closely related to T-cell-mediated immune responses (Pesce et al., 2006; Wynn, 2004), and the regulatory effect of MSCs on T lymphocyte proliferative capability confers them attractive candidates for antifibrotic treatment (Ren et al., 2008). Moreover, autophagy is imperative for both survival and immune function of CD4⁺ and CD8⁺ T lymphocytes (Jia et al., 2015). In this regard, the roles of autophagy played in the immunosuppressive properties of MSCs were exploited. Our results showed that transplanted MSCs were selectively recruited to the fibrotic portal area in the liver. Furthermore, sh*Becn1*-MSCs obviously promoted the immunosuppressive capability of MSCs in CD4⁺ and CD8⁺ T lymphocyte proliferation. This finding suggested that the inhibitive effect of sh*Becn1*-MSCs on infiltration of CD4⁺ and CD8⁺ T lymphocytes might partially account for the elevated antifibrotic effects on the fibrotic liver. Our study corroborated previous research by Ding et al. (2014), who showed that autophagy alleviates kidney fibrosis by regulating TGF-β1 expression. However, one study showed that MSCs exert immunosuppressive effects in CD4⁺ T lymphocytes via TGF-β1 secretion and activation of autophagy (Gao et al., 2016). The cause for this discrepancy may be associated with the molecular interplay between autophagy and immunity; indeed, autophagy functions in both activation and inactivation of immune signaling, thus balancing immune responses (Saitoh & Akira, 2010). Moreover, these discrepancies may be related to differences in the study designs, including tissue and species origins, cell isolation methods, T cell/MSC ratios, cell culture conditions, and time of data analysis.

The therapeutic effects of MSCs in inflammatory diseases is largely due to their unique capacity to secrete immunoregulatory factors (Ranganath, Levy, Inamdar, & Karp, 2012). Moreover, the colocalization of exogenous MSCs, T lymphocytes, and HSCs in the portal fibrotic area in CCl₄-induced fibrotic livers indicated that the inhibition of exogenous sh*Becn1*-MSCs on proliferative capacity of HSCs and T lymphocytes might affect their immunosuppressive

capability via a paracrine pathway, but not via hepatocyte regeneration. PGE_2 is an inflammation-induced immunosuppressive agent secreted by MSCs, which mediates MSC-dependent inhibition on T lymphocytes (M. Bai et al., 2018). Notably, we found that knockdown of *Becn1* suppressed inflammation-induced autophagy and generated more $PTGS2/PGE_2$ in MSCs, consistent with other studies. As outlined by Dang et al. (2014) cytokine-induced autophagy affects the immunomodulatory properties of MSCs via the reactive oxygen species/mitogen-activated protein kinase 1/3/PTGS2 pathway. Additionally, a study by O'Brien et al. (2014) also confirmed that acutely decompensated cirrhosis patients with reduced concentrations of serum PGE_2 displayed attenuated immune function and increased risk of infection. However, the immunomodulatory factors secreted by MSCs are highly changeable, likely because of their vigorous interactions with components of the immune system (Alfaifi et al., 2018). MSCs can secrete various immunoinhibitive cytokines, including indoleamine 2,3-dioxygenase, IL-6, nitric oxide, and IL-10

(Shi et al., 2012). Therefore, we believe that there are other molecules involved in the mechanisms through which sh*Becn1*-MSCs modulate T cells and PGE_2, and these factors should be investigated in the future. Blocked autophagy may cause cellular senescence (Ma et al., 2018) and increase the risk of tumor formation (Aita et al., 1999; Levy et al., 2014; Qu et al., 2003; Wang et al., 2019). Autophagy levels are significantly reduced in aging bone marrow MSCs. In turn, elevated activity of autophagy can partially reverse this senescence and restore bone loss in aged mice. Under certain conditions, loss of the *Becn1* gene in mice promotes tumorigenesis (Qu et al., 2003). In many human tumors, including breast, ovarian, and prostate cancers, the *Becn1* gene is often partially deleted (Aita et al., 1999). These findings indicate that controlling the autophagic activity by genetic manipulation may affect the stem-like characteristics and differentiation functions of MSCs and increase the risk of tumor formation. Therefore, in future studies, it will be necessary to develop a safe and stable method for regulating autophagy.
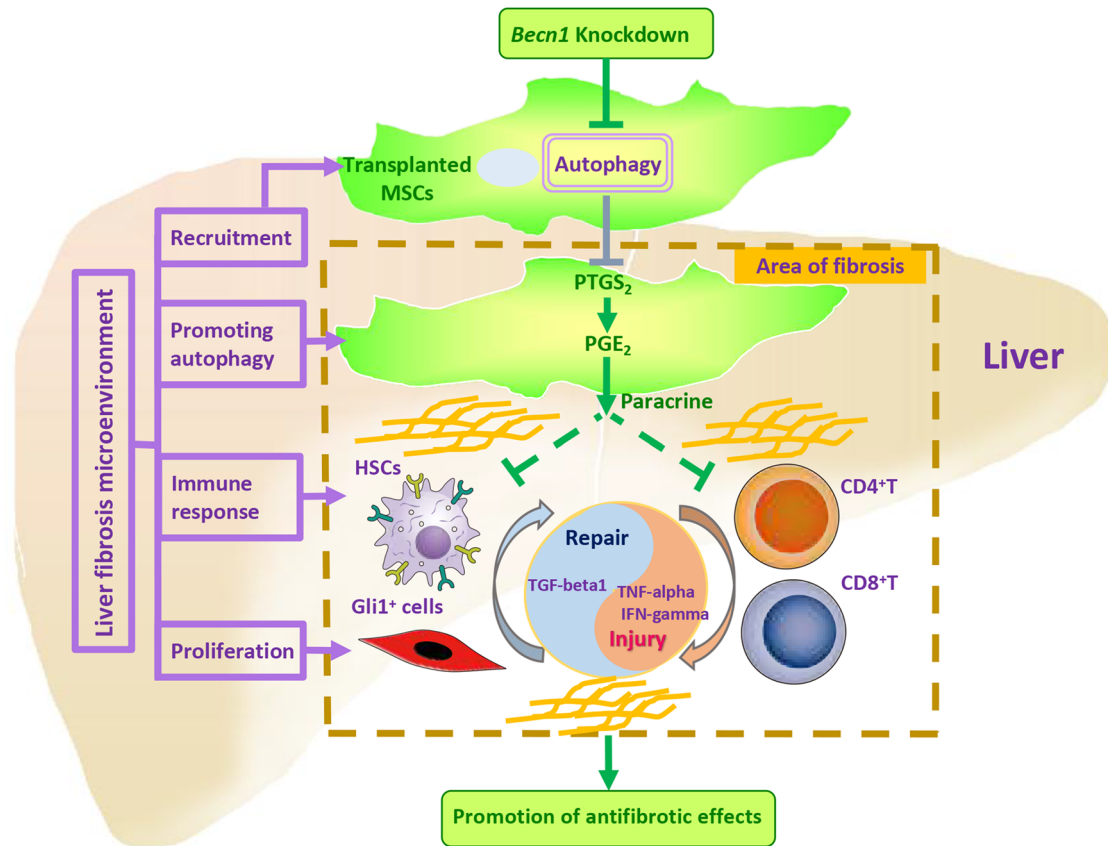

FIGURE 7 Schematic illustration of the proposed model depicting how autophagy suppression enhanced the antifibrotic effect of mesenchymal stem cells (MSCs) under the context of liver fibrosis (LF). LF involves chronic inflammation-induced parenchymal cell injury and activation of consequent repair processes executed by primed myofibroblasts progenitors. Based on our findings, the transplanted MSCs undergo autophagy in the LF microenvironment, and counteracting the microenvironment-induced autophagy by *Becn1* knockdown promotes the antifibrotic effects of MSCs on CCl_4-induced LF. The enhanced antifibrotic potential primed by autophagy inhibition in MSCs may be attributed to their dual inhibitory effects on $CD4^+$ and $CD8^+$ T lymphocyte infiltration and hepatic stellate cells (HSCs) and $Gli1^+$ cell proliferation, which may be regulated by elevated paracrine secretion of $PTGS2/PGE_2$. PGE_2, prostaglandin E_2; PTGS2, prostaglandin-endoperoxide synthase 2

5 | CONCLUSIONS

In summary, our results confirmed, for the first time, that the LF microenvironment impeded the antifibrotic effects of MSCs by inducing autophagy. However, counteracting microenvironment-induced autophagy promoted the antifibrotic effect of MSCs in CCl$_4$-induced LF. The boosted antifibrotic potential primed by autophagy inhibition in MSCs may be attributed to their suppressive effect on CD4$^+$ and CD8$^+$ lymphocytes infiltration and HSCs proliferation, which were regulated by elevated PTGS2/PGE$_2$ via a paracrine pathway. Our data support autophagy as a putative new therapeutic target for MSC-based remedy in LF and other inflammatory disorders (Figure 7).

CONFLICT OF INTERESTS

The authors declare that there are no conflict of interests.

AUTHOR CONTRIBUTIONS

Conceived and designed the experiments: Y. L. L. Performed the experiments: H. Y. W., J. S., C. L., W. H. L., F. M. D., J. W., Y. M., K. A. H., L. N. G., D. H. K., and Q. L. Analyzed the data: Y. L. L., J. S., C. L., H. Y. W., and W. H. L. Wrote the paper: Y. L. L., J. S., H. Y. W., and C. L. All authors read and approved the final version of the manuscript.

DATA ACCESSIBILITY

The data that support the findings of this study are available from the corresponding author upon reasonable request.

ORCID

Can Li http://orcid.org/0000-0002-5746-6368

REFERENCES

Aita, V. M., Liang, X. H., Murty, V. V., Pincus, D. L., Yu, W., Cayanis, E., ... Levine, B. (1999). Cloning and genomic organization of beclin 1, a candidate tumor suppressor gene on chromosome 17q21. *Genomics*, *59*, 59–65. https://doi.org/10.1006/geno.1999.5851

Alfaifi, M., Eom, Y. W., Newsome, P. N., & Baik, S. K. (2018). Mesenchymal stromal cell therapy for liver diseases. *Journal of Hepatology*, *68*, 1272–1285. https://doi.org/10.1016/j.jhep.2018.01.030

Antonioli, M., Di Rienzo, M., Piacentini, M., & Fimia, G. M. (2017). Emerging mechanisms in initiating and terminating autophagy. *Trends in Biochemical Sciences*, *42*, 28–41. https://doi.org/10.1016/j.tibs.2016.09.008

Bai, L., Lennon, D. P., Caplan, A. I., DeChant, A., Hecker, J., Kranso, J., ... Miller, R. H. (2012). Hepatocyte growth factor mediates mesenchymal stem cell-induced recovery in multiple sclerosis models. *Nature Neuroscience*, *15*, 862–870. https://doi.org/10.1038/nn.3109

Bai, M., Zhang, L., Fu, B., Bai, J., Zhang, Y., Cai, G., ... Chen, X. (2018). IL-17A improves the efficacy of mesenchymal stem cells in ischemic-reperfusion renal injury by increasing Treg percentages by the COX-2/PGE2 pathway. *Kidney International*, *93*, 814–825. https://doi.org/10.1016/j.kint.2017.08.030

Cadwell, K. (2016). Crosstalk between autophagy and inflammatory signaling pathways: Balancing defence and homeostasis. *Nature Reviews Immunology*, *16*, 661–675. https://doi.org/10.1038/nri.2016.100

Clarke, A. J., & Simon, A. K. (2018). Autophagy in the renewal, differentiation and homeostasis of immune cells. *Nature Reviews Immunology*, *19*, 170–183. https://doi.org/10.1038/s-41577-018-0095-2

Consentius, C., Reinke, P., & Volk, H. D. (2015). Immunogenicity of allogeneic mesenchymal stromal cells: What has been seen in vitro and in vivo? *Regenerative Medicine*, *10*, 305–315. https://doi.org/10.2217/rme.15.14

Dang, S., Xu, H., Xu, C., Cai, W., Li, Q., Cheng, Y., ... Zhang, Y. (2014). Autophagy regulates the therapeutic potential of mesenchymal stem cells in experimental autoimmune encephalomyelitis. *Autophagy*, *10*, 1301–1315. https://doi.org/10.4161/auto.28771

Deretic, V. (2012). Autophagy: An emerging immunological paradigm. *Journal of Immunology*, *189*, 15–20. https://doi.org/10.4049/jimmunol.1102108

Ding, Y., Kim, S. I., Lee, S. Y., Koo, J. K., Wang, Z., & Choi, M. E. (2014). Autophagy regulates TGF-β expression and suppresses kidney fibrosis induced by unilateral ureteral obstruction. *Journal of the American Society of Nephrology*, *25*, 2835–2846. https://doi.org/10.1681/ASN.2013101068

Djavaheri-Mergny, M., Amelotti, M., Mathieu, J., Besançon, F., Bauvy, C., Souquère, S., ... Codogno, P. (2006). NF-kappaB activation represses tumor necrosis factor-alpha-induced autophagy. *Journal of Biological Chemistry*, *281*, 30373–30382. https://doi.org/10.1074/jbc.M602097200

Fujio, K., Komai, T., Inoue, M., Morita, K., Okamura, T., & Yamamoto, K. (2016). Revisiting the regulatory roles of the TGF-β family of cytokines. *Autoimmunity Reviews*, *15*, 917–922. https://doi.org/10.1016/j.autrev

Gao, L., Cen, S., Wang, P., Xie, Z., Liu, Z., Deng, W., ... Shen, H. (2016). Autophagy improves the immunosuppress on of CD4+ T cells by mesenchymal stem cells through transforming growth factor-β1. *Stem Cells Translational Medicine*, *5*, 1496–1505. https://doi.org/10.5966/sctm.2015-0420

Ge, Y., Huang, M., & Yao, Y. M. (2018). Autophagy and proinflammatory cytokines: Interactions and clinical implications. *Cytokine and Growth Factor Reviews*, *43*, 38–46. https://doi.org/10.1016/j.cytogfr

Ghavami, S., Cunnington, R. H., Gupta, S., Yeganeh, B., Filomeno, K. L., Freed, D. H., ... Dixon, I. M. C. (2015). Autophagy is a regulator of TGF-β1-induced fibrogenesis in primary human atrial myofibroblasts. *Cell Death & Disease*, *6*, e1696. https://doi.org/10.1038/cddis.2015.36

Han, X., Yang, Q., Lin, L., Xu, C., Zheng, C., Chen, X., ... Shi, Y. (2014). Interleukin-17 enhances immunosuppression by mesenchymal stem cells. *Cell Death and Differentiation*, *21*, 1758–1768. https://doi.org/10.1038/cdd.2014.85

Hao, J., Li, S., Shi, X., Qian, Z., Sun, Y., Wang, D., ... Piao, F. (2018). Bone marrow mesenchymal stem cells protect against n-hexane-induced neuropathy through beclin 1-independent inhibition of autophagy. *Scientific Reports*, *8*, 4516. https://doi.org/10.1038/s41598-018-22857-x

Horton, J. A., Hudak, K. E., Chung, E. J., White, A. O., Scroggins, B. T., Burkeen, J. F., & Citrin, D. E. (2013). Mesenchymal stem cells inhibit cutaneous radiation-induced fibrosis by suppressing chronic inflammation. *Stem Cells*, *31*, 2231–2241. https://doi.org/10.1002/stem.1483

Jia, W., He, M. X., McLeod, I. X., Guo, J., Ji, D., & He, Y. W. (2015). Autophagy regulates T lymphocyte proliferation through selective degradation of the cell-cycle inhibitor CDKN1B/p27Kip1. *Autophagy*, *11*, 2335–2345. https://doi.org/10.1080/15548627.2015.1110666

Kramann, R., Schneider, R. K., DiRocco, D. P., Machado, F., Fleig, S., Bondzie, P. A., ... Humphreys, B. D. (2015). Perivascular gli1(+) progenitors are key contributors to injury-induced organ fibrosis. *Cell Stem Cell*, *16*, 51–66. https://doi.org/10.1016/j.stem.2014.11.004

Lee, Y. A., Wallace, M. C., & Friedman, S. L. (2015). Pathobiology of liver fibrosis: A translational success story. *Gut*, *64*, 830–841. https://doi.org/10.1136/gutjnl-2014-306842

Levy, J. M., Thompson, J. C., Griesinger, A. M., Amani, V., Donson, A. M., Birks, D. K., ... Thorburn, A. (2014). Autophagy inhibition improves chemosensivity in BRAF(V600E) brain tumors. *Cancer Discovery*, *4*, 773–780. https://doi.org/10.1158/2159-8290.CD-14-0049

Liu, T., Xu, L., Wang, C., Chen, K., Xia, Y., Li, J., ... Guo, C. (2018). Alleviation of hepatic fibrosis and autophagy via inhibition of transforming growth factor-β1_Smads pathway through shikonin. *Journal of Gastroenterology and Hepatology*, *34*, 263–276. https://doi.org/10.1111/jgh.14299

Liu, Y., Wang, L., Kikuiri, T., Akiyama, K., Chen, C., Xu, X., ... Shi, S. (2011). Mesenchymal stem cell-based tissue regeneration is governed by recipient T lymphocytes via IFN-γ and TNF-α. *Nature Medicine*, *17*, 1594–1601. https://doi.org/10.1038/nm.2542

Ma, Y., Qi, M., An, Y., Zhang, L., Yang, R., Doro, D. H., ... Jin, Y. (2018). Autophagy controls mesenchymal stem cell properties and senescence during bone aging. *Aging Cell*, *17*, e12709. https://doi.org/10.1111/acel.12709

Meng, X. M., Nikolic-Paterson, D. J., & Lan, H. Y. (2016). TGF-β1: The master regulator of fibrosis. *Nature Reviews Nephrology*, *12*, 325–338. https://doi.org/10.1038/nrneph.2016.48

Mougiakakos, D., Jitschin, R., Johansson, C. C., Okita, R., Kiessling, R., & Le Blanc, K. (2011). The impact of inflammatory licensing on heme oxygenase-1-mediated induction of regulatory T cells by human mesenchymal stem cells. *Blood*, *117*, 4826–4835. https://doi.org/10.1182/blood-2010-12-324038

O'Brien, A. J., Fullerton, J. N., Massey, K. A., Auld, G., Sewell, G., James, S., ... Gilroy, D. W. (2014). Immunosuppression in acutely decompensated cirrhosis is mediated by prostaglandin E2. *Nature Medicine*, *20*, 518–524. https://doi.org/10.1038/nm.3516

Pesce, J., Kaviratne, M., Ramalingam, T. R., Thompson, R. W., Urban, J. F., Jr., Cheever, A. W., ... Wynn, T. A. (2006). The IL-21 receptor augments Th2 effector function and alternative macrophage activation. *Journal of Clinical Investigation*, *116*, 2044–2055. https://doi.org/10.1172/JCI27727

Puche, J. E., Saiman, Y., & Friedman, S. L. (2013). Hepatic stellate cells and liver fibrosis. *Comprehensive Physiology*, *3*, 1473–1492. https://doi.org/10.1002/cphy.c120035

Qu, X., Yu, J., Bhagat, G., Furuya, N., Hibshoosh, H., Troxel, A., ... Levine, B. (2003). Promotion of tumorigenesis by heterozygous disruption of the beclin 1 autophagy gene. *Journal of Clinical Investigation*, *112*, 1809–1820. https://doi.org/10.1172/JCI20039

Ranganath, S. H., Levy, O., Inamdar, M. S., & Karp, J. M. (2012). Harnessing the mesenchymal stem cell secretome for the treatment of cardiovascular disease. *Cell Stem Cell*, *10*, 244–258. https://doi.org/10.1016/j.stem.2012.02.005

Ren, G., Zhang, L., Zhao, X., Xu, G., Zhang, Y., Roberts, A. I., ... Shi, Y. (2008). Mesenchymal stem cell mediated immunosuppression occurs via concerted action of chemokines and nitric oxide. *Cell Stem Cell*, *2*, 141–150. https://doi.org/10.1016/j.stem.2007.11.014

Rocheteau, P., Chatre, L., Briand, D., Mebarki, M., Jouvion, G., Bardon, J., ... Chrétien, F. (2015). Sepsis induces long-term metabolic and mitochondrial muscle stem cell dysfunction amenable by mesenchymal stem cell therapy. *Nature Communications*, *6*, 10145. https://doi.org/10.1038/ncomms10145. https://dx.d-oi.org/

Saitoh, T., & Akira, S. (2010). Regulation of innate immune responses by autophagy-related proteins. *Journal of Cell Biology*, *189*, 925–935. https://doi.org/10.1083/jcb.20-1002021

Seki, E., & Schwabe, R. F. (2015). Hepatic inflammation and fibrosis: Functional links and key pathways. *Hepatology*, *61*, 1066–1079. https://doi.org/10.1002/hep.27332

Shi, Y., Hu, G., Su, J., Li, W., Chen, Q., Shou, P., ... Ren, G. (2010). Mesenchymal stem cells: A new strategy for immunosuppression and tissue repair. *Cell Research*, *20*, 510–518. https://doi.org/10.1038/cr.2010.44

Shi, Y., Su, J., Roberts, A. I., Shou, P., Rabson, A. B., & Ren, G. (2012). How mesenchymal stem cells interact with tissue immune responses. *Trends in Immunology*, *33*, 136–143. https://doi.org/10.1016/j.it.2011.11.004

Shibutani, S. T., Saitoh, T., Nowag, H., Münz, C., & Yoshimori, T. (2015). Autophagy and autophagy-related proteins in the immune system. *Nature Immunology*, *16*, 1014–1024. https://doi.org/10.1038/ni.3273

Swart, J. F., de Roock, S., Hofhuis, F. M., Rozemuller, H., van den Broek, T., Moerer, P., ... Wulffraat, N. M. (2015). Mesenchymal stem cell therapy in proteoglycan induced arthritis. *Annals of the Rheumatic Diseases*, *74*, 769–777. https://doi.org/10.1136/annrheumdis-2013-20414

Trautwein, C., Friedman, S. L., Schuppan, D., & Pinzani, M. (2015). Hepatic fibrosis: Concept to treatment. *Journal of Hepatology*, *62*, S15–S24. https://doi.org/10.1016/j.jhep.2015.02.039

Tsuchida, T., & Friedman, S. L. (2017). Mechanisms of hepatic stellate cell activation. *Nature Reviews Gastroenterology & Hepatology*, *14*, 397–411. https://doi.org/10.1038/nrgastro.2017.38

Tu, S. P., Quante, M., Bhagat, G., Takaishi, S., Cui, G., Yang, X. D., ... Wang, T. C. (2011). IFN-γ inhibits gastric carcinogenesis by inducing epithelial cell autophagy and T-cell apoptosis. *Cancer Research*, *71*, 4247–4259. https://doi.org/10.1158/0008-5472.CAN-10-4009

Wang, Y., Chen, X., Cao, W., & Shi, Y. (2014). Plasticity of mesenchymal stem cells in immunomodulation: Pathological and therapeutic implications. *Nature Immunology*, *15*, 1009–1016. https://doi.org/10.1038/ni.3002

Wang, Y., Xiong, H., Liu, D., Hill, C., Ertay, A., Li, J., ... Lu, X. (2019). Autophagy inhibition specifically promotes epithelial-mesenchymal transition and invasion in RAS-mutated cancer cells. *Autophagy*, *20*, 1–14. https://doi.org/10.1080/15548627.20-19.1569912

Wynn, T. A. (2004). Fibrotic disease and the T(H)1/T(H)2 paradigm. *Nature Reviews Immunology*, *4*, 583–594. https://doi.org/10.1038/nri1412

Yuan, Y., Ding, D., Zhang, N., Xia, Z., Wang, J., Yang, H., ... Li, B. (2018). TNF-α induces autophagy through ERK1/2 pathway to regulate apoptosis in neonatal necrotizing enterocolitis model cells IEC-6. *Cell Cycle*, *17*, 1390–1402. https://doi.org/10.1080/15384101.2018.1482150

SUPPORTING INFORMATION

Additional supporting information may be found online in the Supporting Information section.

How to cite this article: Wang HY, Li C, Liu WH, et al. Autophagy inhibition via *Becn1* downregulation improves the mesenchymal stem cells antifibrotic potential in experimental liver fibrosis. *J Cell Physiol.* 2020;235:2722–2737. https://doi.org/10.1002/jcp.29176